3D Scene Generation from Scene Graphs and Self-Attention

Pietro Bonazzi[1], Mengqi Wang[1], Diego Martin Arroyo[2], Fabian Manhardt[2], Federico Tombari[2]
[1]University of Zürich, [2]Google

ABSTRACT

Synthesizing realistic and diverse indoor 3D scene layouts in a controllable fashion opens up applications in simulated navigation and virtual reality. As concise and robust representations of a scene, scene graphs have proven to be well-suited as the semantic control on the generated layout. We present a variant of the conditional variational autoencoder (cVAE) model to synthesize 3D scenes from scene graphs and floor plans. We exploit the properties of self-attention layers to capture high-level relationships between objects in a scene, and use these as the building blocks of our model. Our model, leverages graph transformers to estimate the size, dimension and orientation of the objects in a room while satisfying relationships in the given scene graph. Our experiments shows self-attention layers leads to sparser (HOW MUCH) and more diverse scenes (HOW MUCH)Încluded in this work, we publish the first large-scale dataset for conditioned scene generation from scene graphs, containing over XXX rooms (of floor plans and scene graphs).

1 INTRODUCTION

With the growing popularity of immersive virtual worlds in AR/VR and other graphics applications, there has been increased demand for automated 3D realistic content creation, including 3D scene generation [31, 8]. Instead of labor-intensive 3D scene modeling by human, automated procedural methods for synthesizing indoor environments are beneficial for many real-world applications like simulated navigation and interior design. Deep generative models are used widely and showed promising results in interior scene layout generation task by predicting the location, dimension and orientation of each object in the room [15, 21, 30, 17, 19]. Furthermore, to allow users to have more fine-grained control over the objects in the scene, conditional layout generation uses various types of conditions, such as text descriptions [32], floor plans [19, 27], semantic maps [29] and scene graphs [5, 17]. As a compact and robust representation of a scene, scene graphs are shown to be an effective and user-friendly tool to manipulate the generated scene [6, 5].

1.1 Motivation

Even conditioned on scene graphs, our scene synthesis is not limited in a deterministic way because scene graphs are a high-level abstract description, which can maps to potentially infinite number of valid scenes. To keep the stochastic nature of the generated scene layout, Variational Autoencoder (VAE) [12] formulation is commonly used in scene generation [5, 17, 19], due to its capability of modeling high dimensional distributions. To the best of our knowledge, current available VAE models for this task either use Graph Convolutional Networks (GCNs) as building blocks of VAE [5, 17] or use other data structure such parse tree, hierarchical scene structures or sequence data as inputs [21, 15, 19, 27]. Even though GCNs have shown to be one of the most effective neural network architectures on graph datasets [24, 23], later works have revealed the attention mechanism [2] great potentials for processing not only sequence data in the field of natural language processing (NLP) [33], but also graph-based data in molecules and social networks for node classification and graph regression task [7, 18] with competitive or superior performance against GCNs. In particular, model with self-attention blocks have demonstrated better performance than GCN-based models [1] in document layout generation.

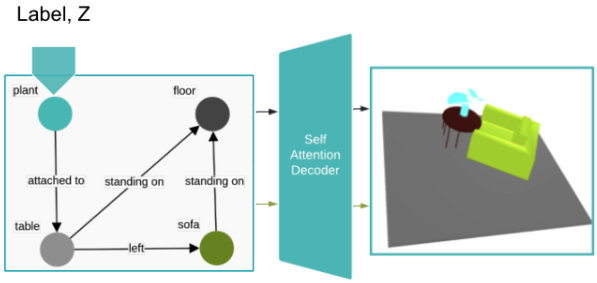

Figure 1 Inference Pipeline

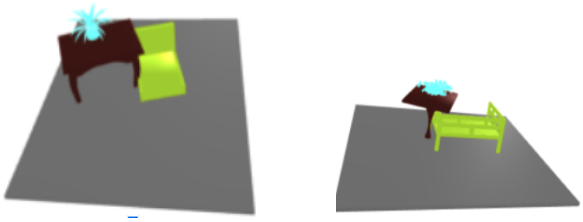

Figure 2 Given a sampled vector z, our attention-based conditional VAE model produces various scene layouts constraint on the source scene graph.

In this paper, we propose an attention-based architecture within the VAE framework, designed for graph-based data structure and trained for 3D scene generation from scene graphs. Inspired by [7], we explore design choices of attention mechanism on graphs - *e.g.* including vs. excluding edge features (relation type) in attention computation, applying learned vs. non-learned prior, etc. Due to the nature that scene graphs are commonly not fully connected with implicit relations that are not indicated by connected components [4], self-attention mechanism is a suitable candidate for discovering implicit relations between objects in a given graph without explicit supervision.

To summarize, our main contributions are:

- The first cVAE architecture with self-attention layers as fundamental building blocks, tailored to 3D scene generation from scene graphs.
- Exploration of strategies for attention module designed for graph data structure.

2 RELATED WORK

In this section, we summarize the research area and the state-of-the-art in the field of end-to-end scene generation.

Graph-based Scene Synthesis. A number of studies [36, 21, 15, 35, 17, 5] model 3D scene descriptions with graph-based data structures, in particular, through parse trees [21], adjacency matrices [35], scene graphs [36, 17, 5] and scene hierarchies [15].

To synthesize scenes conditioned on graph data, researchers have designed method based on message passing modules [36], complete spatial randomness (CSR) [34] and VAE [21, 15, 35, 27, 17, 5]. In particular, the VAE framework has been extended with grammar rules one-hot-encoding [21], recursive neural network [15], feed-forward neural network [35] and GCN [27, 17, 5].

Sequence-based Scene Synthesis. In contrast to graph-based approaches, a new line of work [22, 30, 19] models a room as a sequence of objects associated with their semantic labels and 3D oriented bounding boxes (OBBs).

These models employ a CNN-based architecture [22] or transformer-based architectures [30] [19] to directly learn the distribution of the data without conditioning the output on object relationships.

Outside the field of scene generation, self-attention [1] has effectively surpassed VAE architecture based of GNN [14] in the task of document layout generation, while also treating documents sections as a flatten sequence.

Across the field of scene generation only few architectures [30, 19, 5] do not capitalize on additional supervision and post processing optimization techniques to obtain realistic scenes.

Among these, we value scene graphs as an intermediate representation for its potential in expressing higher-level visual understanding and meaning. Therefore, we try to capitalize on recent successes presented by transformer-based architectures [19, 1] and improve the state-of-the-art [5] for scene generation conditioned on scene graphs.

3 METHODOLOGY

In this paper , we present a new method to generate the layout of a 3D scene conditioned on a scene graph. We define scene graph $G(O, E)$ as a set of nodes $o_i \in O$, where $i = 1, ..N$ and N is the number of nodes in G. We express the connection between nodes as edges $e_{ij} \in E$. Edges are directional semantic descriptions of relationships between pair of nodes. Nodes are the semantic labels of objects in the scene.

Following previous work on VAE [21, 15, 35, 27, 17, 5], we encode node spatial attributes and edge labels , to generate 3D scenes constrained on graph relationships. Our architecture is summarized in Figure 3.

In section 3, we summarize the steps we performed to encode the nodes and edges before the self-attention mechanism. Next, in paragraph 3 we review the method to obtain the node position with Laplacian eigenvectors. In section 3, we explain three encoder methods to apply the self-attention operator on graphs. From this, in 3, we demonstrate the sampling process and provide an overview of the decoding pipeline. Finally, in Section 3, we review the loss function minimized during training.

Data preparation. The spatial attributes of each node are expressed in terms of size s_i (i.e. height, width and length of the OBB), 3D coordinates of the object centroid l_i and rotation r_i of the object around the z-axis.

The first part of the architecture transforms the size s, location l, z-aligned object angular rotation r and the object class label c of all the objects o belonging to the scene graph G to a coded form.

It must be noted that objects with 359 degrees of rotation have a similar orientation with others orientated at zero degree angle. Therefore, we treat r as a categorical variable and one-hot-encode it in 24 bins. We apply the same mapping technique to the labels in c.

After these steps, we linearly transform the attributes to four distinct embedding with 16 dimensions each. Next, we concatenate to obtain a shared embedding X for all nodes in G .

$$X = s \oplus l \oplus r \oplus c \in \mathbb{R}^{4n} \tag{1}$$

Separately, we also encode E as the class label feature of the edges e, applying the same procedure explained previously for c .

Consequently, we apply the activation function RELU on the learned embedding X and E to learn complex patterns in the data, support sparsity and reduce the likelihood of vanishing gradients.

Laplacian Positional Encoding. Before the self-attention operator, we modify the node embedding X by adding structural graphical position information of each object. We used the Laplacian ($\mathcal{L}_p$) eigenvector as positional encoding [3, 7], because it can be derived as a generalization of the positional encoding used in the original Transformer architecture [25].

$$X = X + \mathcal{L}_p(G) \tag{2}$$

Graph Convolution Networks (GNN). A Graph Convolutional Network (GCN) allows information to flow between the connected objects of the graph . We use GNN as auxiliary modules before the self-attention layers. Similary to [5], we pass direct triplets of the type $[X_{src}, E, X_{dst}]$ to a MultiLayer Perceptron (MLP) where X_{src} means the node embedding of the source nodes and X_{dst} refers to the node embedding of the destination nodes. Next, we aggregate the information coming from both direction to the respective nodes using summation. Finally, we update the node features using another MLP layer.

Graph Self-Attention models. As shown in 4, we tested three design of Graph self-attention encoders and decoders.

In our first design, GNNA, we linearly transform the node embedding X for each object sequentially after two GNN layers, to obtain the Query Q, Key K and Value V needed in the self-attention [25]. We separate the embedding in 8 heads for numerical stability and we pass the resulting weighted vector through a feed-forward-network with residuals.

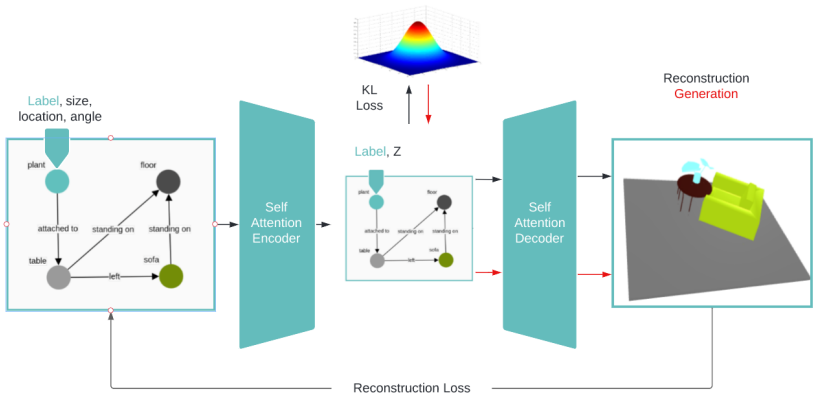

Figure 3 . Architecture diagram. Given a scene graph G and a floor plan F, our model scale, locate and orient the OBB of each object. Through our self-attention encoder, we learn a distribution in the latent space. Sampling from this learned underlying distribution enable our attention-based decoder to reconstruct the original layout or generate a new one. Finally, we retrieve the 3D models to match the shape of the generated OBBs.

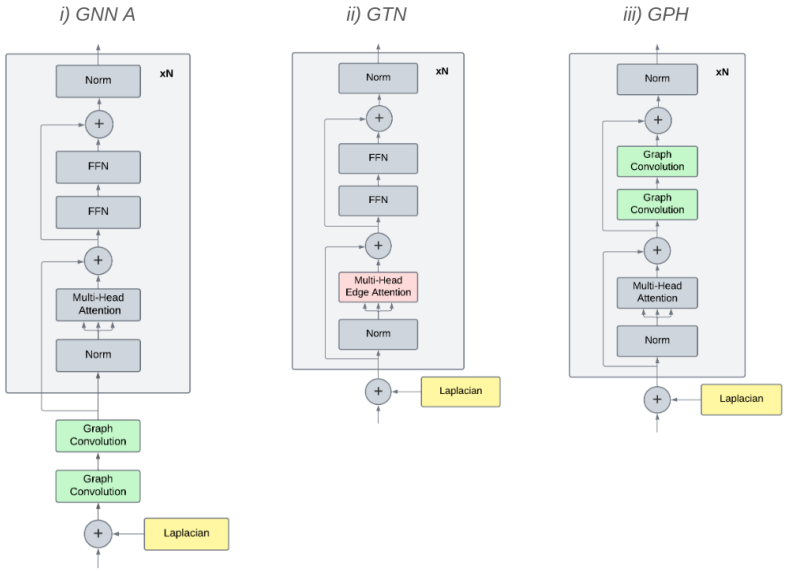

Figure 4 . Self-Attention Encoder/Decoders. We test three methods to incorporate graph information in the self-attention mechanism.

In the second design, GTN, we compute self-attention by leveraging edge level attention with connected nodes [7]. Through this system, the attention score of isolated nodes is not be computed. To avoid this and better regularize the boundary of the scene , we decided to add a special central node with whom every object has an incoming edge. Attention is computed on an edge level by re-projecting source X_{src} and destination X_{dst} nodes embedding to the edges. The edge feature E is used to adjust the attention score before the softmax . Finally, we aggregate the weighted V only on the destination nodes.

In conclusion , we tested an extension of the Graphormer [16] architecture, called GPH, which integrates Laplacian Positional Encoding before the attention mechanism.

Figure 5 . Special Node. We experimented by adding to the input scene graph a node representing the floorplan connected to all other nodes. We obtained the node embedding using a pre-trained finetuned ResNet50.

Special node computation. To better regularize on the boundary of the scene, we introduce the floor plan as an additional condition along with the scene graph. Floor plans are extracted followed by the methods explained in section 4. Floor plan images are encoded by a pre-trained ResNet50 [9] with a trained final feed-forward layer. Another advantage of adding the special node to the graph is avoiding edge-less graphs, which are problematic in edge-level attention computation. The steps are summarized in Figure 5.

Latent space, reparametrization and decoding. The outcome of the self-attention layers are compressed with an MLP to approximate the mean μ and logarithmic variance $logvar$ of a distribution $(q(z\|x))$ for node and edges in the graphs.

To make the gradients of our model differentiable with back propagation, we use the well-known reparameterization trick. The random node z is obtained by addying to the newly introduced parameter the learned μ and by multiplying it with the approximated $logvar$.

Training objective. VAE makes it possible to model the intractable posterior distribution of our data $(p(z\|x))$. Our model learns to fit a distribution $(q(z\|x))$ to a Gaussian by optimizing the lower bound on the marginal likelihood (the ELBO) [12] typically used in variational autoencoders.

In detail, our cost function is composed of two terms : the reconstruction term $\mathcal{L}_r$ and the Kullback–Leibler (KL) divergence loss $\mathcal{L}_{KL}$.

$\mathcal{L}_{KL}$ measures the distance between the approximated distribution learned by our model $(q(z\|x))$ and a Gaussian distribution $(p(z))$ used instead of the true posterior $(p(z\|x))$. Formally we expressed this term as follows :

$$\mathcal{L}_{KL} = D_{KL}(q(z|x), ||p(z)) \tag{3}$$

The reconstruction term $\mathcal{L}_r$ is a sum of mean square error distances and cross entropy loss (CE). We use the L2 loss to compute the distance between the predicted size and the original measurements of volume. The L2 loss is also used to compute the difference between the predicted location and the true centroid coordinates. The cross entropy loss is only computed over the 24 classes of orientation.

$$\mathcal{L}_r = \|\hat{l} - l\|_2 + CE(\hat{r}, r) + \|\hat{s} - s\|_2 \tag{4}$$

To reduce the risk of posterior collapse [10], we weight the KL term with a $\beta = 0.01$. The final training objective equation looks as follows :

$$\mathcal{L} = \mathcal{L}_r + \beta\mathcal{L}_{KL} \tag{5}$$

Implementation details. We trained our model using Pytorch [20], Deep Graph Library[28] and Nvidia Quadro RTX 8000 for acceleration. We use multi-head attention with 8 heads to stabilize the predictions. We trained 2 self-attention layers. We optimized the weights of our model using the Adam's algorithm [11] with a batch size of 64 for 100 epochs.

4 EXPERIMENTS

Dataset. Our model is trained on the 3DSSG dataset [26], a semi-automatically generated dataset with dense semantic graph annotations. It features 1482 scene graphs generated from real-world 3D scans, with 48k object nodes and 544k edges in total. There are 534 object classes and 40 object relations types in the dataset. The 3DSSG dataset also provides a cleaner version with smaller subgraphs of 4–9 nodes, split from the original dense graphs. In this subset version, only 26 relationships and 160 common object instances are remained.

As an extension of the 3DSSG dataset, [5] implemented an annotation pipeline to obtain canonical tight bounding boxes per instance. OOBs are represented with 7 parameters, i.e. 3 for size, 3 for translation as well as 1 for the rotation around the z-axis since most objects are supported by a horizontal surface. To clarify, OOBs information is only used in the training process.

Along with scene graph, 2D binary floor plans are also used as the condition for our generative model. To get the floor plan, we tested two methods to process the 3D point clouds. The first set of floor plan is computed as top-down orthographic projection of point clouds, smoothed with common morphological operations including dilation/erosion and opening/closing. Another method to get more regularized floor plan is projecting OOBs to the xy-plane, with post-processing of small OBBs that are outside of the floor object. We observe no significant differences in model performance using the first method or the second method, so we used silhouettes from OBBs for floor plans.

We trained and evaluated our model on the official splits in 3DSSG dataset [26].

Evaluation metrics. Since scene generation is a one-to-many task, meaning multiple possible results for the same input, we evaluate the layout both qualitatively and quantitatively, in terms of accuracy and diversity.

We define accuracy as meeting the constraints imposed by the input scene graph and floor plan. Typical metrics for measuring location and dimension predictions, such as L1/L2 norm are not suitable for one-to-many tasks, due to the strict comparison between the predictions and the ground truth. Similar to [17, 5], we recompute geometric relationships from the generated layouts to measure if the input relationships are fulfilled.

To better visualize the spatial distribution of inter-object relationships, Table 1 visualizes heatmaps of the ground truth and predicted bounding box distributions, inspired by [6]. Spatially

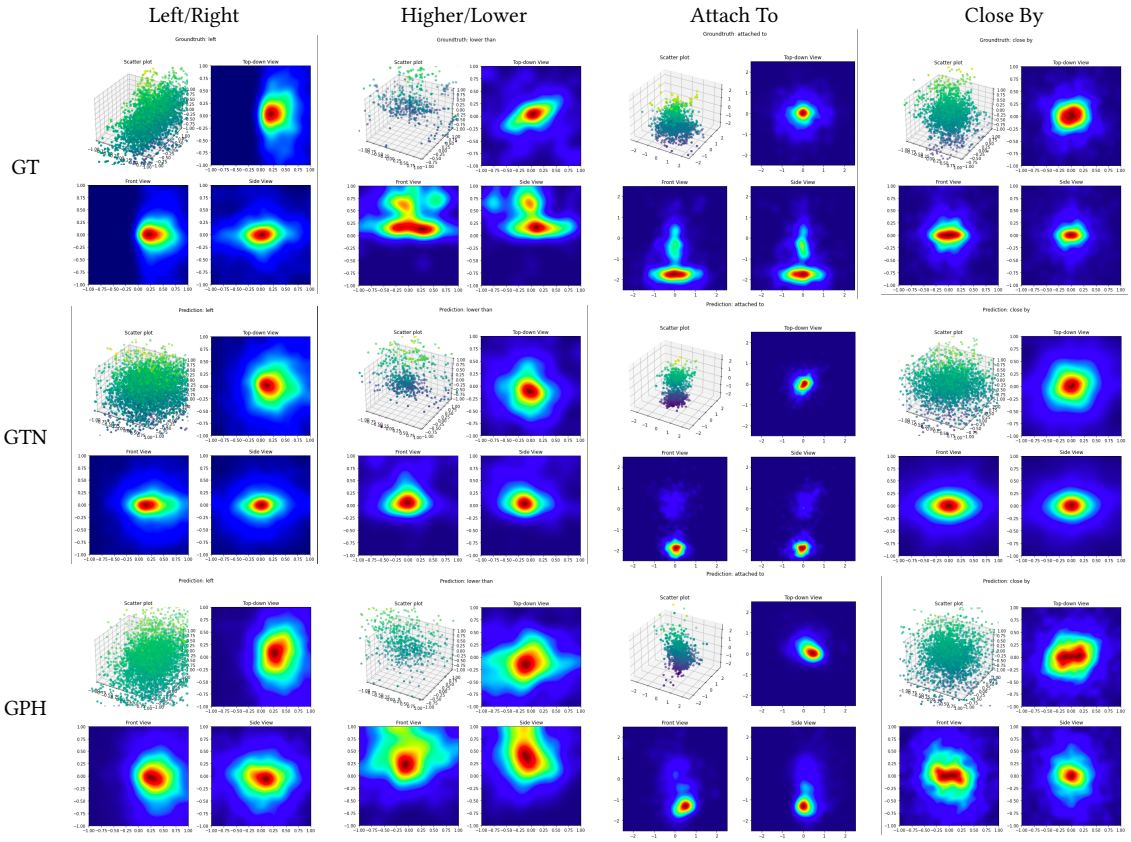

Table 1 Heatmaps generated from object and subject relative positions for selected relationship types. 4 views in each relationship from top left to bottom right are 3D scatter plot, top-down view (orthographic projection on xy-plane), front view (orthographic projection on xz-plane), side view (orthographic projection on yz-plane).

well-constrained relationships that can indicate the spatial distributions are selected, such as left/right, higher/lower, attached to. For every triplet (i.e. subject - predicate - object) in the validation set we predict the subject and object 3D location coordinates. From there, the relative position between the object and subject centers can be computed, then grouped by relationship category. We observe similar distributions from either edge-based GTN or node-based Graphomer with the groundtruth distributions generated from validation dataset. It indicates that our models have learned to accurately capture spatial relationships to predict relative locations between objects.

Diversity is measured by the standard deviation among 10 samples that are generated under the same scene graph and its floor plan. We compute this metric separately for dimension, location in meters and angle in degrees, and compute the mean over the evaluation set.

Quantitative results. Table 2 and 3 show comparisons with different baselines (Graph-to-box and Graph-to-3D [5]) in terms of accuracy and diversity. Graph-to-box [5] is trained only on layout, as a ablation for Graph-to-3D [5] without the sharing of layout and shape. We include it because shape features are not included in our models so it is a more fair comparisons. As indicated in [5], Graph-to-3D performs better than Graph-to-box, but our models still show competitive or superior performance against Graph-to-3D even without shape features.

	Mean	L/R	F/B	S/B	H/L
3D-SLN[17]	0.76	0.74	0.69	0.77	0.85
GraphTo3D[5]	0.89	0.81	0.81	**0.99**	**0.98**
GNN + L	0.92	0.87	0.91	0.96	0.93
GNNA + L	0.91	0.94	0.82	0.98	0.90
GPH	0.85	0.79	0.84	0.89	0.87
GPH + L	**0.92**	**0.94**	**0.94**	0.91	0.89

Table 2 Precision Results: L/R (Left/Right), F/B (Front/Behind), S/B (Smaller/Bigger), H/L (Higher, Lower). Laplancian Encoding (L) improves precision results.

	Size	Location	Rotation
3D-SLN[17]	0.03	0.06	11.83
GraphTo3D[5]	0.10	0.49	**20.53**
GNN + L	**0.79**	0.42	12.27
GNNA + L	0.78	0.43	16.32
GPH	0.78	0.49	20.0
GPH + L	0.77	0.36	14.73

Table 3 Diversity Results

Qualitative results. We show qualitative results of rendered scene in Figure 6, as well as a qualitative comparison with existing methods in Table 4. In alignment with the quantitative results, we observe that our approach yield diverse layouts that follows the given scene graph. Compared to Graph-to-3D [5], our models can generate more plausible layout with fewer volume overlapping even without shape features.

5 CONCLUSION AND FUTURE WORK

This work proposes the first cVAE architecture with self-attention layers as fundamental building blocks, tailored to 3D scene generation from scene graphs. We showed that both diverse and plausible layouts can be generated from our methods. However, we also note that our proposals can still be improved in promising future researches. One interesting direction would be extending the scene graph connectivity with concepts like k-hop graphs [13], since we observed many failure cases are due to the lack of connection edges in the input graphs.

REFERENCES

[1] Diego Martin Arroyo, Janis Postels, and Federico Tombari. "Variational Transformer Networks for Layout Generation". In: 2021.
[2] Dzmitry Bahdanau, Kyunghyun Cho, and Yoshua Bengio. *Neural Machine Translation by Jointly Learning to Align and Translate*. 2014. DOI: 10.48550/ARXIV.1409.0473. URL: https://arxiv.org/abs/1409.0473.
[3] Mikhail Belkin and Partha Niyogi. "Laplacian Eigenmaps for Dimensionality Reduction and Data Representation". In: *Neural Computation* 15.6 (2003), pp. 1373–1396. DOI: 10.1162/089976603321780317.
[4] Xiaojun Chang et al. "A Comprehensive Survey of Scene Graphs: Generation and Application". In: *IEEE Transactions on Pattern Analysis and Machine Intelligence* (2022), pp. 1–1. DOI: 10.1109/tpami.2021.3137605. URL: https://doi.org/10.1109%2Ftpami.2021.3137605.
[5] Helisa Dhamo et al. "Graph-to-3D: End-to-End Generation and Manipulation of 3D Scenes using Scene Graphs". In: *IEEE International Conference on Computer Vision (ICCV)*. 2021.
[6] Helisa Dhamo et al. *Semantic Image Manipulation Using Scene Graphs*. 2020. DOI: 10.48550/ARXIV.2004.03677. URL: https://arxiv.org/abs/2004.03677.
[7] Vijay Prakash Dwivedi and Xavier Bresson. "A Generalization of Transformer Networks to Graphs". In: *AAAI Workshop on Deep Learning on Graphs: Methods and Applications* (2021).
[8] Matthew Fisher, Manolis Savva, and Pat Hanrahan. "Characterizing Structural Relationships in Scenes Using Graph Kernels". In: *ACM SIGGRAPH 2011 Papers*. SIGGRAPH '11. Vancouver, British Columbia, Canada: Association for Computing Machinery, 2011. ISBN: 9781450309431. DOI: 10.1145/1964921.1964929. URL: https://doi.org/10.1145/1964921.1964929.
[9] Kaiming He et al. *Deep Residual Learning for Image Recognition*. 2015. DOI: 10.48550/ARXIV.1512.03385. URL: https://arxiv.org/abs/1512.03385.
[10] Irina Higgins et al. "beta-VAE: Learning Basic Visual Concepts with a Constrained Variational Framework". In: *5th International Conference on Learning Representations, ICLR 2017, Toulon, France, April 24-26, 2017, Conference Track Proceedings*. 2017.
[11] Diederik P. Kingma and Jimmy Ba. *Adam: A Method for Stochastic Optimization*. 2014. DOI: 10.48550/ARXIV.1412.6980. URL: https://arxiv.org/abs/1412.6980.
[12] Diederik P. Kingma and Max Welling. "Auto-Encoding Variational Bayes". In: 2014.
[13] Sukhamay Kundu and Subhashis Majumder. "A Linear Time Algorithm for Optimal K-Hop Dominating Set of a Tree". In: *Inf. Process. Lett.* 116.2 (Feb. 2016), pp. 197–202. ISSN: 0020-0190. DOI: 10.1016/j.ipl.2015.07.014. URL: https://doi.org/10.1016/j.ipl.2015.07.014.
[14] Hsin-Ying Lee et al. "Neural Design Network: Graphic Layout Generation with Constraints". In: (Dec. 2019).
[15] Manyi Li et al. "GRAINS: Generative Recursive Autoencoders for INdoor Scenes". In: *ACM Trans. Graph.* (2019).
[16] Kevin Lin, Lijuan Wang, and Zicheng Liu. "Mesh Graphormer". In: *ICCV*. 2021.
[17] Andrew Luo et al. "End-to-End Optimization of Scene Layout". In: *Proceedings of the IEEE/CVF Conference on Computer Vision and Pattern Recognition*. 2020, pp. 3754–3763.
[18] Erxue Min et al. *Masked Transformer for Neighhourhood-aware Click-Through Rate Prediction*. 2022. DOI: 10.48550/ARXIV.2201.13311. URL: https://arxiv.org/abs/2201.13311.
[19] Despoina Paschalidou et al. "ATISS: Autoregressive Transformers for Indoor Scene Synthesis". In: *Advances in Neural Information Processing Systems (NeurIPS)*. 2021.
[20] Adam Paszke et al. "PyTorch: An Imperative Style, High-Performance Deep Learning Library". In: *Advances in Neural Information Processing Systems 32*. Ed. by H. Wallach et al. Curran Associates, Inc., 2019, pp. 8024–8035. URL: http://papers.neurips.cc/paper/9015-pytorch-an-imperative-style-high-performance-deep-learning-library.pdf.
[21] Pulak Purkait, Christopher Zach, and Ian Reid. "SG-VAE: Scene Grammar Variational Autoencoder to Generate New Indoor Scenes". In: 2020, pp. 155–171.
[22] Daniel Ritchie, Kai Wang, and Yu-An Lin. "Fast and Flexible Indoor Scene Synthesis via Deep Convolutional Generative Models". In: *Proceedings of the IEEE/CVF Conference on Computer Vision and Pattern Recognition (CVPR)*. June 2019.
[23] Alvaro Sanchez-Gonzalez et al. *Learning to Simulate Complex Physics with Graph Networks*. 2020. DOI: 10.48550/ARXIV.2002.09405. URL: https://arxiv.org/abs/2002.09405.
[24] Michael Schlichtkrull et al. *Modeling Relational Data with Graph Convolutional Networks*. 2017. DOI: 10.48550/ARXIV.1703.06103. URL: https://arxiv.org/abs/1703.06103.
[25] Ashish Vaswani et al. "Attention is all you need". In: 2017.
[26] Johanna Wald et al. "Learning 3D Semantic Scene Graphs from 3D Indoor Reconstructions". In: *Conference on Computer Vision and Pattern Recognition (CVPR)*. 2020.
[27] Kai Wang et al. "PlanIT: Planning and Instantiating Indoor Scenes with Relation Graph and Spatial Prior Networks". In: *ACM Trans. Graph.* (2019).
[28] Minjie Wang et al. "Deep Graph Library: A Graph-Centric, Highly-Performant Package for Graph Neural Networks". In: *arXiv preprint arXiv:1909.01315* (2019).
[29] Ting-Chun Wang et al. *High-Resolution Image Synthesis and Semantic Manipulation with Conditional GANs*. 2017. DOI: 10.48550/ARXIV.1711.11585. URL: https://arxiv.org/abs/1711.11585.
[30] Xinpeng Wang, Chandan Yeshwanth, and Matthias Nießner. "SceneFormer: Indoor Scene Generation with Transformers". In: *arXiv preprint arXiv:2012.09793* (2020).
[31] Lap-Fai Yu et al. "Make It Home: Automatic Optimization of Furniture Arrangement". In: *ACM Trans. Graph.* 30.4 (July 2011). ISSN: 0730-0301. DOI: 10.1145/2010324.1964981. URL: https://doi.org/10.1145/2010324.1964981.
[32] Han Zhang et al. *StackGAN: Text to Photo-realistic Image Synthesis with Stacked Generative Adversarial Networks*. 2016. DOI: 10.48550/ARXIV.1612.03242. URL: https://arxiv.org/abs/1612.03242.
[33] Jiawei Zhang et al. "Graph-Bert: Only Attention is Needed for Learning Graph Representations". In: *arXiv preprint arXiv:2001.05140* (2020).
[34] Song-Hai Zhang et al. "Fast 3D Indoor Scene Synthesis with Discrete and Exact Layout Pattern Extraction". In: (2020).
[35] Zaiwei Zhang et al. "Deep Generative Modeling for Scene Synthesis via Hybrid Representations". In: *ACM Trans. Graph.* (2020).
[36] Yang Zhou, Zachary While, and Evangelos Kalogerakis. "SceneGraphNet: Neural Message Passing for 3D Indoor Scene Augmentation". In: *IEEE Conference on Computer Vision (ICCV)*. 2019.

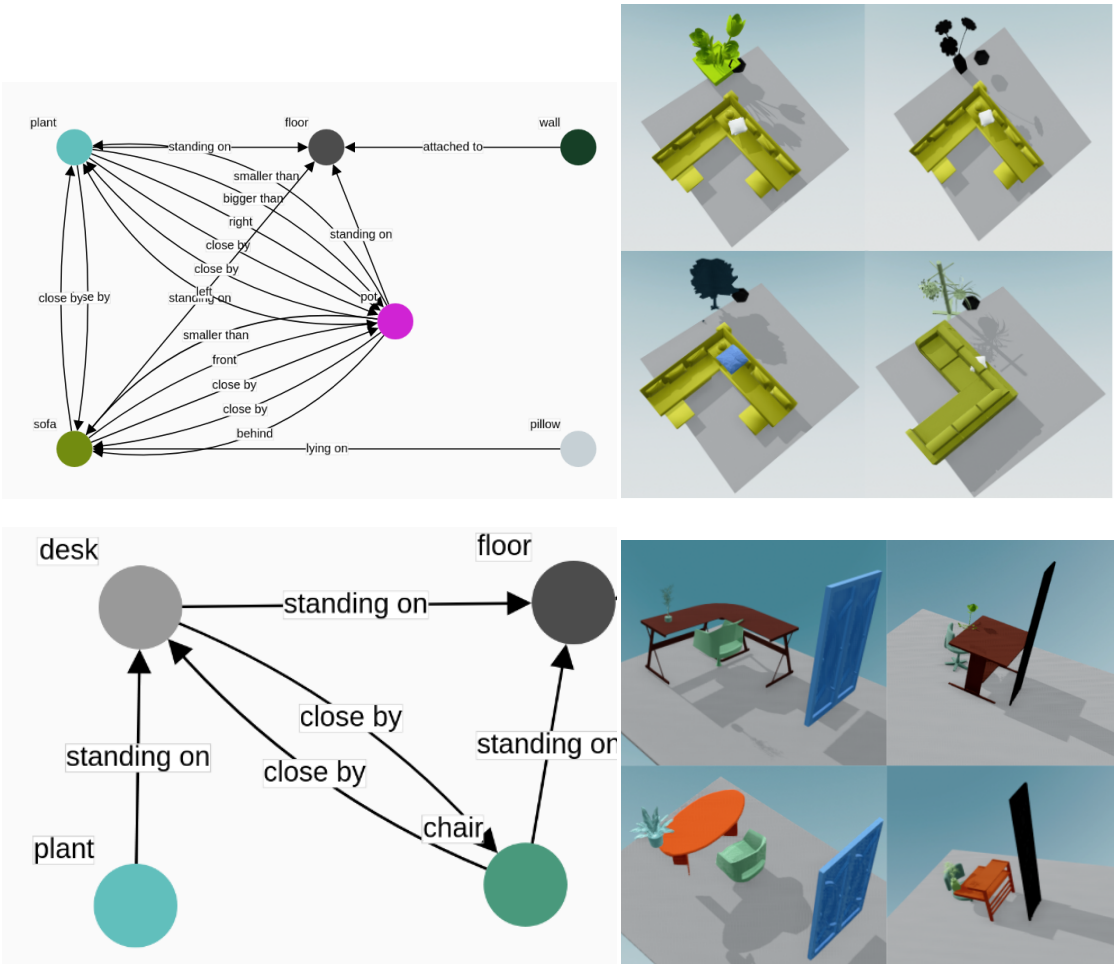

Figure 6 Generated layouts of scene graphs in 3DSSG [26]. Given the same input scene graph, both diverse and plausible layouts are generated from our method. To obtain these scene the covariance was manually scaled.

Mesh	Graph-to-3D	Ours
	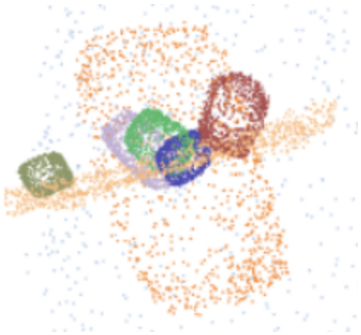	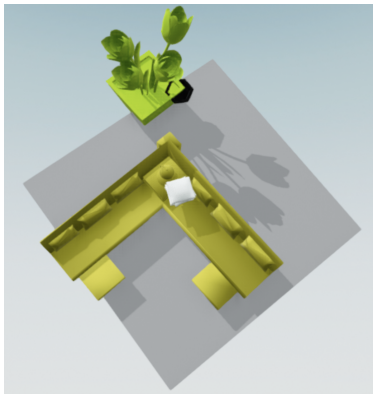
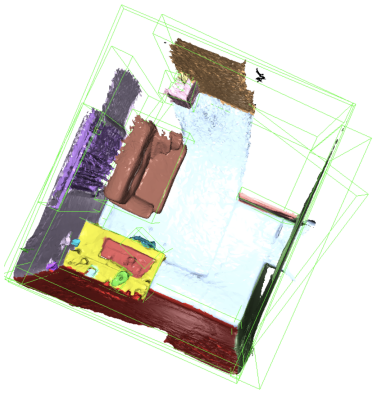	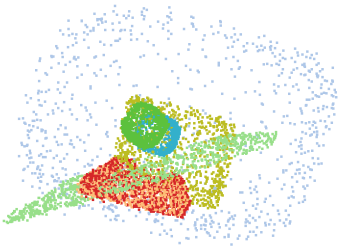	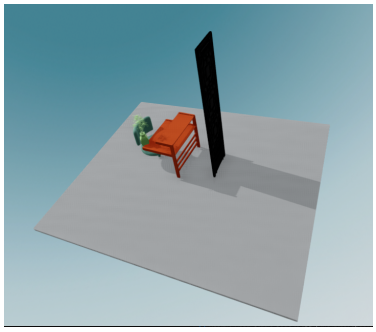

Table 4 Qualitative comparison between Graph-to-3D and our method

Mesh	ShapeNet	Graph-to-3D	Graph-to-3D+Attention	
				
				

Table 5 Generation results